ANALYSIS OF PLUME EXTENT USING ANALYTICAL SOLUTIONS FOR CO_2 STORAGE

JAN M. NORDBOTTEN[1,2], MICHAEL A. CELIA[2]

[1] *Department of Mathematics, University of Bergen, Bergen, Norway*
[2] *Department of Civil and Environmental Engineering, Princeton University, NJ, USA*

ABSTRACT

The evaluation of possible leakage pathways from CO_2 storage operations requires attention to the magnitude, concentration and timescales involved. Herein we discuss a problem related to CO_2 storage, the migration of CO_2 as it is injected. This is accomplished through the application of analytical solutions. In particular, we derive a new analytical insight into the problem of fluid injection into a confined aquifer, which gives us analytically the furthest extent of the injected fluid (CO_2), as well as the extent of the region in which the formation fluid (brine) has evaporated into the injected fluid. We apply these new analytical solutions to a hypothetical injection case based on data from Alberta, Canada, and discuss the results in terms of the surprising variability in observed system responses. We conclude this paper by emphasizing the value of analytical solutions both in semi-analytical frameworks and as benchmarks for numerical simulations.

1. INTRODUCTION

Anthropogenic carbon emissions are generally considered to play an important role in the development of the earth's climate (International Panel on Climate Change 2005). As a way of reducing these emissions, injection of CO_2 into deep saline aquifers has been identified as one of the most promising options based on practical, social and economical considerations (Bruant et al 2002, Pacala and Socolow 2004). Understanding the complex nature of multiphase flow is a prerequisite for assessing the impact of potential storage operations. Herein we will exploit some recent developments in the mathematical treatment of the governing equations for two-phase flow to assess the injection phase of possible injection scenarios.

Nordbotten et al. (2005b) investigated the spreading of CO_2 during injection based on an energy minimization approach. Their investigation is limited to systems of relatively high injection rates compared to aquifer permeability, height and fluid density difference. A different approach was taken in Huppert and Woods (1995), where similarity solutions were used for systems in which the fluid mobilities could be considered equal. The limitations of both these approaches were overcome in Nordbotten and Celia (2006), where similarity solutions were developed for fluids with different mobilities, and which further allow for phase transfer between the CO_2 and brine.

Herein we will use the theory developed in Nordbotten and Celia (2006) to conduct an investigation on the importance of mass transfer between phases during CO_2 injection. We will focus in particular on the nature of the drying front. This front separates the two-phase

region where brine-saturated CO_2 flows at residual brine saturation from the single-phase region closer to the well, where all residual brine has evaporated.

Motivated by the low values of the gravity number Γ, defined in Section 3, reported for typical injection scenarios in Nordbotten et al (2005b), we will in this investigation consider this quantity negligible, and derive new analytical insight building on the similarity solutions presented in Nordbotten and Celia (2006).

We will structure this presentation as follows: The next section provides an overview and motivation for the choice of data set on which we base this investigation. Section 3 briefly reviews the governing equations, as well as summarizes the main results from Nordbotten and Celia (2006). We then continue with the exposition of the results in Section 4, before the paper concludes with a discussion pertaining both to the insights obtained from this investigation as well as the application of similarity solutions as benchmark solutions for numerical codes.

2. DATA SET FOR EXAMPLE PROBLEMS

Injection of acid gases (mixtures of CO_2 and H_2S) into confined aquifers has a long and well documented history in Alberta, Canada. We will look at a range of conditions here as typical of the environments encountered also for many practical CO_2 sequestration operations.

Nordbotten et al (2005b) identified four end member cases, representing injection into 'deep' and 'shallow' formations, in 'cold' and 'warm' basins. The depths were chosen as 3000 meters and 1000 meters respectively. A lower limit for a 'cold' environment was estimated based on an average surface temperature of 10ºC and a geothermal gradient of 25ºC/km, while the upper limit for a 'warm' aquifer was estimated based on average surface temperatures of 20ºC and a geothermal gradient of 45 ºC/km. This, together with typical salinity ranges taken from the formations in Alberta, led to ranges of the fluid densities and viscosities, given in Table 1. In an interesting study, Spycher et al (2003) investigated the phase partitioning between CO_2 and water. While not strictly applicable to the problem at hand, since we are dealing with brines, we will nevertheless assume that the values reported there give a good indication of the phase partitioning for the saline systems we consider. The mass fraction of CO_2 in water denoted β_1 and the mass fraction of water in brine denoted β_2 are also given in Table 1.

TABLE 1. Fluid properties of CO_2 and brine, taken from Nordbotten et al (2006) and Spycher et al (2003). Values marked with a star (*) are outside the temperature range investigated in the reference, and were estimated based on 110 ºC.

	Cold Shallow	Cold Deep	Warm Shallow	Warm Deep
Temperature (ºC)	35	85	65	155
Pressure (MPa)	10.5	31.5	10.5	31.5
Density CO_2 (kg)	714	733	266	479
Density brine (kg)	1121	1099	1104	1045
Viscosity CO_2 (mPa.s)	0.0577	0.0611	0.023	0.0395
Viscosity brine (mPa.s)	1.19	0.511	0.687	0.254
Mass fraction β_1 (%)	4.9	4.9	3.9	5.1*
Mass fraction β_2 (%)	0.18	0.73	0.27	2.4*

TABLE 2. Flow properties of the formations.

	Sandstone Shallow (Viking 1240 m)	Sandstone Deep (Basal 2732 m)	Carbonate Shallow (Wabamun 1357 m)	Carbonate Deep (Nisku 2049 m)
Residual saturation brine	0.55	0.3	0.6	0.35
Endpoint rel. perm. CO_2	0.35	0.55	0.55	0.2
Permeability (mD)	10	10	50	50
Porosity (%)	10	10	5	5
Thickness (m)	50	50	50	50
Injection rate (Mt/y)	1	1	1	1
Injection time (y)	15	15	15	15

The relative-permeability displacement characteristics of CO_2-brine systems in formations underlying Alberta have been discussed in Bennion and Bachu (2005). We choose four formations studied in their laboratory work as representative of our 'deep' and 'shallow' formations; one sandstone and one carbonate formation of each. The endpoint relative permeability values for CO_2, as well as the residual saturations of brine are given in Table 2. Also included are typical permeability and porosity values (Stefan Bachu, Alberta Energy and Utilities Board, personal communication, 2006). Finally, we complete the description of our case by setting the injection rate to 1 Mt/y. This injection rate is typical of a medium sized power plant, and we will consider the plume evolution after 15 years of operation.

3. GOVERNING EQUATIONS

We will consider flow governed by the standard multiphase extension of Darcy's law, which (under the assumption of negligible capillary pressure) is stated for phase α as

$$q_\alpha = -k\frac{k_{r,\alpha}}{\mu_\alpha}\nabla(p - zg), \tag{1}$$

where q is the Darcy flux, k is the permeability of the medium, k_r is the relative permeability, which is taken as a function of saturation, μ is the fluid viscosity, p is fluid pressure, g is the gravitational constant, z is the vertical coordinate, increasing downward, and $\alpha = c, cw, w$ denote the dry CO_2, wet CO_2, and brine, respectively. Mass conservation for each fluid

$$\frac{\partial}{\partial t}\phi\rho_\alpha S_\alpha + \nabla\cdot q_\alpha = 0, \tag{2}$$

is given in terms of porosity ϕ, density ρ and saturation S. Finally, we close the system with the restriction that the fluids fill the void space, $S_c + S_w = 1$.

We will assume that the injection takes place through a fully penetrating well, with rates and aquifer slope consistent such that the aquifer can be approximated as horizontal for the injection period (Gasda et al 2006). We approximate the brine-CO_2 interface as sharp and given by $z = h(r,t)$, see Figure 1. The saturation points of CO_2 in brine and brine in CO_2 are held constant throughout the system, and the mass fractions at the saturation point are denoted β_1 and β_2 respectively. This leads to an evaporation of the residual brine saturation as dry CO_2 is injected into the formation. We represent this by introducing a drying front, which is the interface $z = i(r,t)$ between the region with dry CO_2 and the region with both wet CO_2 and residual brine saturation.

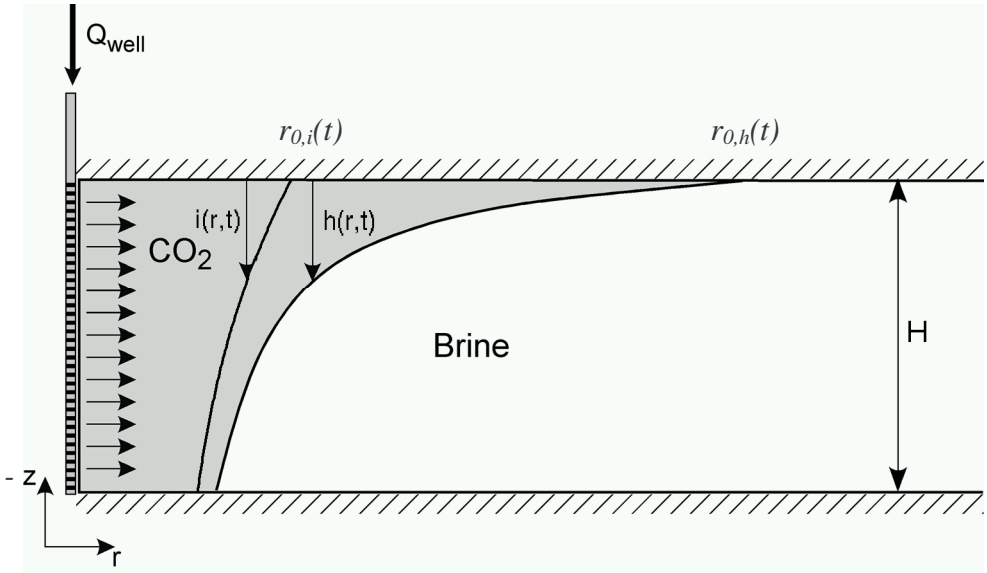

FIGURE 1: Schematic diagram showing a typical plume of injected fluid of thickness h(r,t) trailed by a drying front denoted by i(r,t). The outer extents of h(r,t) and i(r,t) are denoted $r_{0,h}(t)$ and $r_{0,i}(t)$.

3.1 Self similar equations

This problem was studied theoretically in Nordbotten and Celia (2006), where they found that the system scales with a similarity variable of length squared over time. We will here briefly outline the main derivation and assumptions.

As the horizontal length scale of the problem is far greater than the vertical, it is appropriate to assume that the flow is essentially horizontal. This enables us to apply the vertical equilibrium assumption to describe the pressure variation in the vertical direction,

$$p(r,t,0) = p(r,t,H) - (H - h(r,t))\rho_w g - (h(r,t) - i(r,t))\rho_{cw} g - i(r,t)\rho_c g\,. \tag{3}$$

Since this is an approximate relationship, we cannot enforce mass conservation and Darcy flow locally, and we replace equations (1) and (2) with their vertically integrated forms

$$-2\pi r\phi \frac{\partial (H-h)}{\partial t} = \frac{\gamma_1}{1-S_{res}} \frac{\partial Q_w}{\partial r}, \tag{4a}$$

$$-2\pi r\phi \frac{\partial i}{\partial t} = \frac{\gamma_2}{1-S_{res}} \frac{\partial Q_c}{\partial r}, \tag{4b}$$

$$Q_{cw} + Q_c + Q_w = Q_{\text{well}}\,. \tag{4c}$$

where S_{res} denotes residual saturation of the resident brine, and the radially dependent vertically-integrated flow rates Q_α are defined by

$$Q_c = -2\pi r i k \frac{k_{r,c}}{\mu_c} \frac{\partial p_c}{\partial r}, \tag{5a}$$

$$Q_{cw} = -2\pi r (h-i) k \frac{k_{r,cw}}{\mu_{cw}} \frac{\partial p_{cw}}{\partial r}\,. \tag{5b}$$

$$Q_w = -2\pi r (H-h) k \frac{k_{r,w}}{\mu_w} \frac{\partial p_w}{\partial r}\,. \tag{5c}$$

Note that we have introduced radial coordinates and assumed that the problem possesses angular symmetry. In moving from point equations to vertically-averaged equations, we have introduced new variables, where H is the thickness of the formation, Q is the angular and vertically integrated flux as a function of radius r, and the dimensionless phase transfer parameters are given by

$$\gamma_1 = \left[1 + \frac{\beta_1 S_{res}}{(1-S_{res})(1-\beta_2)}\right]^{-1}, \qquad \gamma_2 = \left[1 + \frac{(1-\beta_1) S_{res}}{(1-S_{res})\beta_2}\right]^{-1}, \tag{6}$$

where β_1 and β_2 are as defined previously. We now introduce the dimensionless parameters

$$\Gamma \equiv \frac{2\pi(\rho_w - \rho_{cw}) g k H^2}{Q_{well}\mu_w}, \qquad \lambda_1 \equiv \frac{\mu_w}{\mu_c}, \qquad \lambda_2 \equiv \frac{k_{r,cw}\mu_w}{\mu_{cw}}, \qquad \vartheta = \frac{\rho_{cw} - \rho_c}{\rho_w - \rho_{cw}},$$
$$\chi \equiv \frac{2\pi H \phi (1-S_{res})}{Q_{well}} \frac{r^2}{t}, \qquad h' \equiv \frac{h}{H}, \qquad i' \equiv \frac{i}{H}, \qquad p' \equiv \frac{p}{(\rho_w - \rho_{cw}) g H}, \tag{7}$$

where we refer to the parameter Γ as the gravity number. By combining equations (4) and (5), with the introduction of the dimensionless variables and parameters, we obtain the following, self-similar set of second-order ordinary differential equations:

$$\frac{d}{d\chi} h' = \frac{4\Gamma\gamma_1}{\chi} \frac{d}{d\chi}\left((1-h')\chi \frac{d}{d\chi} p'\right), \tag{8a}$$

$$-\frac{d}{d\chi} i' = \frac{4\gamma_2\Gamma\lambda_1}{\chi} \frac{d}{d\chi}\left(i'\chi \frac{d}{d\chi}(p' + h' + \vartheta i')\right), \tag{8b}$$

$$\frac{d}{d\chi} p' = -\frac{\frac{1}{2\Gamma\chi} + \left(\lambda_2 h' + (\lambda_1 - \lambda_2) i'\right)\frac{d}{d\chi} h' + \lambda_1 i' \vartheta \frac{d}{d\chi} i'}{\lambda_2 (h' - i') + \lambda_1 i + (1-h')}. \tag{8c}$$

These equations are independent of time, and for special cases were shown to be a stable solution to the time dependent equations (4) and (5) in Nordbotten and Celia (2006). Equations (8) are bounded by the conditions that there exists $\chi_{0,h}$ and $\chi_{0,i}$ where $h'(\chi_{0,h})=0$ and $i'(\chi_{0,i})=0$, and that the mass balance integrals

$$\int_0^{\chi_{0,h}} h'(\chi) d\chi = 2\gamma_1 \qquad \text{and} \qquad \int_0^{\chi_{0,i}} i'(\chi) d\chi = 2\gamma_2 \tag{9,10}$$

are satisfied. For the special case where Γ is negligible, corresponding to scenarios with relatively large injection rates, low permeability and/or thin aquifers, Equations (8) degenerate to first order differential equations. If further $\lambda_1 = \lambda_2$, corresponding to end-point relative permeability values for CO_2 near unity, Nordbotten and Celia (2006) gave the analytical solutions

$$h' = \frac{1}{(\lambda_2 - 1)}\left(\sqrt{\frac{2\lambda_2\gamma_1}{\chi}} - 1\right) \qquad i' = \left(\gamma_1 - \lambda_2 \frac{\gamma_2}{\gamma_1}\right)^{-1} \frac{\sqrt{\chi} - \gamma_2\sqrt{2\lambda_2/\gamma_1}}{\sqrt{\chi}}, \tag{11}$$

bounded by $0 \le i' \le h' \le 1$.

Equations (8) will be the main focus of this study.

3.2 Analysis in limit of negligible gravity number

For the data presented in Section 2 we see that the gravity number Γ varies between 0.027 and 0.18, all below the threshold value of Γ=.5 identified in Bachu et al (2005) as the value below which the gravity number is negligible. In this section we will therefore use the limit $\Gamma \to 0$, for which equations (8) become a set of first-order differential equations,

$$\frac{d}{d\chi}h' = -\frac{2\gamma_1}{\chi}\frac{d}{d\chi}\left(\frac{(1-h')}{\lambda_2(h'-i')+\lambda_1 i+(1-h')}\right), \tag{12a}$$

$$\frac{d}{d\chi}i' = \frac{2\gamma_2\lambda_1}{\chi}\frac{d}{d\chi}\left(\frac{i'}{\lambda_2(h'-i')+\lambda_1 i+(1-h')}\right). \tag{12b}$$

Since at the outer tip $\chi_{0,i}$ of the drying front, $i'(\chi_{0,h})=0$, we see from in Equation (12b) that a non-zero derivative of i' can only exist at

$$\chi_{0,i} = \frac{2\lambda_1\gamma_2}{1+(\lambda_2-1)h'}. \tag{13}$$

Further, since for the region $\chi_{0,i} < \chi < \chi_{0,h}$ we have $i'(\chi_{0,h})=0$, such that Equation (12a) degenerates to the analytical solution given in Equation (11). Then by combining Equation (11) and (13) we have that

$$\chi_{0,i} = \max\left(\frac{2\lambda_1^2\gamma_2^2}{\lambda_2\gamma_1}, \frac{2\lambda_1\gamma_2}{\lambda_2}\right). \tag{14}$$

Setting $h' = 0$ in Equation (11) gives the equivalent outer tip of the plume itself

$$\chi_{0,h} = 2\lambda_2\gamma_1. \tag{15}$$

Thus we have obtained analytical expressions for the outermost extent of both interfaces of interest. The plume shapes themselves can be obtained by integration of Equations (12).

4. RESULTS

We have applied the analytical expressions for the extent of the CO_2 plume and the drying front, equations (14) and (15) to the data sets given in Section 2. The analytical results are given in Table 3.

TABLE 3. Outer extent of fluid interfaces

	Sandstones				Carbonates			
	Shallow		Deep		Shallow		Deep	
	Cold	Warm	Cold	Warm	Cold	Warm	Cold	Warm
Plume extent ($\chi_{0,h}$)	13.6	20.0	9.0	6.9	21.1	31.0	3.3	2.5
Drying front extent ($\chi_{0,i}$)	$8.8\cdot10^{-3}$	$1.3\cdot10^{-2}$	$6.4\cdot10^{-2}$	$2.0\cdot10^{-1}$	$4.6\cdot10^{-3}$	$6.8\cdot10^{-3}$	$1.4\cdot10^{-1}$	$4.5\cdot10^{-1}$
Plume extent ($r_{0,h}$) (m)	4499	8923	2895	3139	8405	16690	2556	2770
Drying front extent ($r_{0,i}$) (m)	115	229	244	537	124	247	530	1172
Mobility ratio λ_1	20.1	29.9	8.4	6.4	20.1	29.9	8.4	6.4
Mobility ratio λ_2	7.2	10.5	4.6	3.5	11.3	16.4	1.7	1.3
Gravity number Γ	0.012	0.016	0.026	0.051	0.059	0.079	0.126	0.259

There are several interesting observations to be made from Table 3. Firstly, we note that although the injection rate, injection period and formation thickness are equal for all the cases discussed above, there is still a large variation in the radial spread of the CO_2 plumes. Indeed, while the plume reaches almost 17 km away from the well for the injection into the shallow warm carbonate formation, an equivalent mass injected into a deep, cold carbonate formation does not even propagate one sixth of that distance away from the well. This large variation in plume extent is due to several factors. Since our mass injection rate is constant, the volume injected will be inversely proportional to the density of the CO_2. Further, it is clear from Equation (15) that the outer plume extent in dimensional coordinates is proportional to the mobility ratio between wet CO_2 and brine, such that the outer extent of the plume in dimensional coordinates is proportional to the square root of this mobility ratio. Finally, the volume available for sequestration varies significantly between the formations, with effective porosity for the wet CO_2 (the product of porosity and $(1\text{-}S_{res})$, the saturation of CO_2 at residual brine saturation) varying more than a factor 3; from 2% in the shallow carbonate formations to 7% in the deep sandstone formations.

Another interesting point relating to the results in Table 3 is the relative minor extent of the drying front. We see that for the deep warm carbonate formations we have a drying front extending slightly more than 1150 meters out from the well, which is about four tenths of the extent of the whole CO_2 plume for this case. However, this is by far the end member case, with drying front interfaces in the shallow formations not reaching 250 meters, less than three percent of the outermost tip of the plumes.

The final line in Table 3 gives the density parameter for the system. As discussed above, Bachu et al (2005) found that this parameter is negligible when Γ is smaller than 0.5, which is the case for all eight cases considered in the table. Therefore the use of Equations (14) and (15) to obtain the outer points of the fluid interfaces is justifiable.

5. DISCUSSION

While numerical methods are invaluable in modeling and predicting system behavior, we have seen above that simple analytical solutions can still provide insight into complex problems. In particular, our analytical treatment has shown that the presence of a drying front has no impact on the outer extent of the CO_2 migration during injection, as seen from Equation (15). Further, the extent of the region of dry CO_2 for a wide range of conditions relevant to CO_2 injection appears to be negligible. This observation is particularly interesting in the perspective of the integrity of abandoned wells, since it is known that wet CO_2 is corrosive to steel casing, and as such may open conduits for leakage.

We note that recent research has attempted to use analytical and semi-analytical solutions to parts of the problem of CO_2 leakage through abandoned wells during an injection operation, and devise overall estimates for the flow of CO_2 during the injection phase (Nordbotten et al 2005a, Kavetski et al 2006). These semi-analytical solution procedures aim at obtaining fast and accurate solutions, at a minimum computational effort. Thus one has the opportunity to spend computational power on multiple realizations, and obtain probability distributions relating the risk and magnitude of leakage, as functions of the uncertainties in the input parameters of the system. This approach is explored in the context of a hypothetical injection site in Alberta in Kavetski et al (2006).

The solutions presented herein are valuable in the setting of semi-analytical solutions, as they provide simple algebraic expressions for crucial parameters such as maximum plume spread, taking into account physical processes such as phase transitions. Such expressions have not previously been available. Further, similarity equations such as those given in equations (8) are very useful, since the solution of these equations give the shape of a CO_2 plume, not only at a particular time, but for all time, given that the properties of the system (such as injection rate) do not change. Thus significant computation savings are possible.

We conclude this discussion by pointing out the obvious advantage of having a wide variety of analytical solutions available for validation of numerical simulators and codes. The approximations involved in obtaining equations (8) can in many cases be shown to be negligible in the limit of late time. Thus, the solution of equations (8), which can easily be obtained to high precision, can provide a benchmark for numerical solutions to equations (1) and (2). Such a comparison was performed in Nordbotten et al (2005b), as well as in Bachu et al (2005), using the industry standard numerical reservoir simulator Eclipse, showing excellent agreement over a range of parameters.

ACKNOWLEDGEMENTS

This work was supported in part by BP and Ford Motor Company through funding to the Carbon Mitigation Initiative at Princeton University. The authors are also grateful to Stefan Bachu for many interesting discussions, and for providing comments on an earlier version.

BIBLIOGRAPHY

Bachu, S., Nordbotten, J. N., Celia, M. A. 2005, *Evaluation of the spread of acid gas plumes injected in deep saline aquifers in western Canada as an analogue to CO2 injection in continental sedimentary basins*, In: Proceedings of 7th International Conference on Greenhouse Gas Control Technologies. *Volume 1: Peer-Reviewed Papers and Overviews* (E.S.Rubin, D.W.Keith and C.F.Gilboy, eds.), Elsevier, 479-487, 2005.

Bruant, R.G., Guswa, A.J., Celia, M.A., & Peters, C.A. 2002 "Safe Storage of Carbon Dioxide in Deep Saline Aquifers", *Environmental Science and Technology*, June 1, 241A-245A.

Bennion, B. and Bachu, S. 2005 *Relative Permeability Characteristics for Supercritical CO2 Displacing Water in a Variety of Potential Sequestration Zones in the Western Canada Sedimentary Basin*, SPE Paper 95547.

Gasda, S. E., Celia, M. A. and Nordbotten, J. M. 2006 *Significance of dipping angle on CO_2 plume migration in deep saline aquifers*, In Proceedings of the 16th conference on Computational Methods in Water Resources.

International Panel on Climate Change 2005 *Special Report on Carbon Dioxide Capture and Storage.*

Huppert, H. E. & Woods, A. W. 1995 Gravity driven flows in porous layers. *J. Fluid Mech.* **292**, 55-69.

Kavetski, D., Nordbotten, J. M, and Celia, M. A. 2006 *Analysis of potential CO2 leakage through abandoned wells using a semi-analytical model*, In Proceedings of the 16th conference on Computational Methods in Water Resources.

Nordbotten J. M., Celia M. A. 2006, *Similarity solutions for fluid injection into confined aquifers*, to appear in Journal Fluid Mechanics.

Nordbotten, J. M., Celia, M. A., Bachu, S. & Dahle, H. K. 2005a Semi-analytical solution for CO_2 leakage through an abandoned well. *Env. Sci. and Tech.* **39**(2), 602-611.

Nordbotten, J. M., Celia, M. A. & Bachu, S. 2005b Injection and storage of CO_2 in deep saline aquifers: Analytical solution for CO_2 plume evolution during injection. *Transp. Porous Media*, **55**, 339-360.

Pacala, S. & Socolow, R. 2004 Stabilization wedges: Solving the climate problem for the next 50 years with current technologies. *Science* **305**(5684), 968-972.

Spycher N., Pruess K. and Ennis-King J. 2003, CO_2-H_2O mixtures in the geological sequestration of CO_2. I. Assessment and calculation of mutual solubilities from 12 to 100 degrees C and up to 600 bar. Geochima and Cosmochima acta **67**(16), 3015-3031.